 ICES-2017-256

Four Bed Molecular Sieve – Exploration (4BMS-X) Virtual Heater Design and Optimization

R. Gregory Schunk[1] and Warren T. Peters[2]
NASA Marshall Space Flight Center, Huntsville, Alabama 35812

John T. Thomas, Jr.[3]
Jacobs ESSSA Team, Huntsville, Alabama 35812

A 4BMS-X (Four Bed Molecular Sieve – Exploration) design and heater optimization study for CO_2 sorbent beds in proposed exploration system architectures is presented. The primary objectives of the study are to reduce heater power and thermal gradients within the CO_2 sorbent beds while minimizing channeling effects. Some of the notable changes from the ISS (International Space Station) CDRA (Carbon Dioxide Removal Assembly) to the proposed exploration system architecture include cylindrical beds, alternate sorbents and an improved heater core. Results from both 2D and 3D sorbent bed thermal models with integrated heaters are presented. The 2D sorbent bed models are used to optimize heater power and fin geometry while the 3D models address end effects in the beds for more realistic thermal gradient and heater power predictions.

Nomenclature

2D	=	Two Dimensional
3D	=	Three Dimensional
4BMS-X	=	Four Bed Molecular Sieve - Exploration
AES	=	Advanced Exploration Systems
α	=	Thermal Diffusivity ($k/\rho C_p$)
CDRA	=	Carbon Dioxide Removal Assembly
CO_2	=	Carbon Dioxide
C_p	=	Specific Heat
C	=	Wall Void Fraction Constant
ECLS	=	Environmental Control and Life Support
ε, ε_∞	=	Void Fraction, Bulk Void Fraction
h	=	Convective Heat Transfer Coefficient or (k/L)
ISS	=	International Space Station
k, k_{eff}	=	Thermal Conductivity, Effective Thermal Conductivity
LSS	=	Life Support Systems
N	=	Wall Void Fraction Exponent
NASA	=	National Aeronautics and Space Administration
psia	=	pounds per square inch absolute
Q''	=	Heat Flux
ρ	=	Density
T,T_∞	=	Temperature, Bulk Temperature
τ	=	Time

[1] Technical Assistant, Thermal Analysis and Control Branch/EV34
[2] Aerospace Engineer, Environmental Control and Life Support Development Branch/ES62
[3] Senior Mechanical Engineer, Environmental Control and Life Support Development Branch/ES62

I. Introduction

THE NASA ISS (International Space Station) Exploration Office is dedicated to the advancement and development of closed loop ECLS (Environmental Control and Life Support) technologies pursuant to future crewed space exploration. A CO_2 technology development roadmap for exploration has been formulated to advance both existing and new technologies to an on-orbit evaluation via an ISS flight demonstration early in the next decade.[1] As part of the development process, the 4BMS-X will introduce a number of potential improvements over existing ISS CDRA (Carbon Dioxide Removal Assembly) technology including cylindrical sorbent beds for better packing efficiency and containment and an improved heater core. Multiple heater designs, including finned cartridge heaters and flexible Kapton® heaters bonded to thermally conductive face-sheets, are considered in this study. Cartridge heaters will permit higher temperature CO_2 desorption or sorbent regeneration from unintended exposure to water vapor which may be advantageous for some sorbents. Kapton heaters will have a lower allowable use temperature and implementation will be subject to an adhesive suitable for 4BMS-X desorption temperatures.

The primary heater sizing and design requirements established for this study are half cycle time, target temperature and the desire to minimize thermal gradients and flow channeling. The desired half cycle time is 80 minutes with a heat-up time of 60 minutes to the target temperature of 200 ºC. The target represents an average bed temperature. In the baseline 4BMS-X design the sorbent bed is driven to higher temperature than is necessary to desorb CO2 from zeolite 13X (baseline sorbent) as the sensible energy of the effluent gas is also used to help desorb water vapor from the downstream desiccant bed. A modification to introduce a heater upstream of the desiccant bed may reduce the sorbent bed target temperature and will be considered in a separate trade. Minimizing thermal gradients in the sorbent bed will increase efficiency as well as potentially mitigate pellet dust formation resulting from thermal expansion. A specific thermal gradient is not defined but a lower temperature limit of 150 ºC in the bed is desired to facilitate CO_2 desorption and an upper limit within +10ºC of the target temperature is desired to mitigate dust formation. Channeling is not quantified in this trade but qualitative assessments on heater fin geometry and surface area that could exacerbate channeling are made.

II. Conceptual 4BMS-X Design

The 4BMS-X (see Figure 1) contains two pelletized adsorbent beds to remove CO_2 respired by the crew. Each CO_2 adsorbent bed is paired with an upstream desiccant bed to condition the inlet air (i.e. remove water vapor) prior to entry into the adsorbent bed. While one adsorbent bed is actively capturing CO_2 at near ambient pressure, the other is regenerated through applied heat under a partial vacuum. Heaters and associated fins span the length of the adsorbent beds with flow through axial cavities formed by the fins and the outer container. The 4BMS-X sorbent beds are filled with spherical zeolite 13X (Grace Davison 544) pellets with a nominal diameter of 2.19 mm.[2] The fins facilitate heat transfer from embedded heaters during CO_2 desorption. Wall effects may be apparent several pellet diameters into the channel domain as increased bed porosity near the wall may affect flow distribution, axial pressure drop, lateral heat transfer and adsorbent performance. The phenomenon of increased flow next to the wall due to increased void fraction is known as channeling. Channeling will adversely affect performance due to both the increased flow rate and increased void fraction near solid boundaries such as fins and the external container.

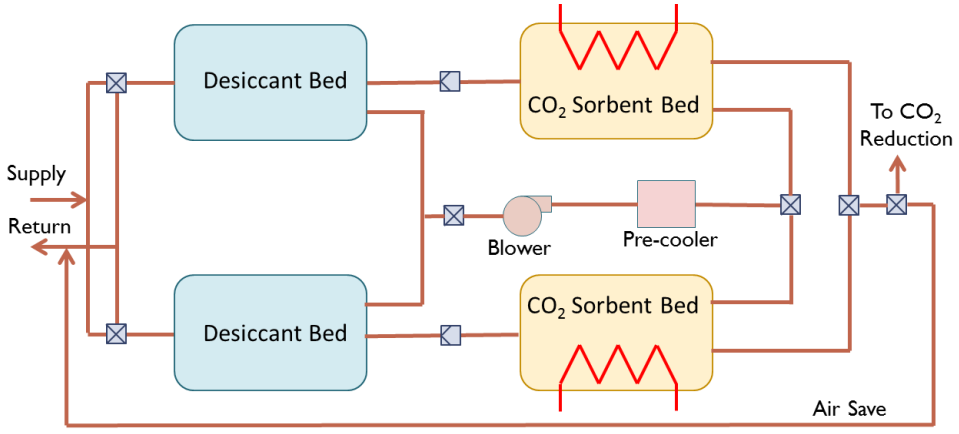

Figure 1. 4BMS-X

A conceptual design for a single 4BMS-X desiccant/sorbent bed pair is shown in Figure 2. The beds are cylindrically shaped following industrial practice for fixed beds to insure the sorbents are fully compacted and to minimize heat transfer to the surroundings.. Each cylindrical housing is constructed from Aluminum 6061 and is comprised of two end caps, mating flanges and a barrel section to contain the sorbent material. The two cylindrical beds are mated together through a common flow path containing a check valve between the beds. Each bed is insulated with a ¾ inch layer of Pyropel LD6[3] thermal insulation. The sorbent bed container is removed to expose the heater core and associated fins in the graphic. The inside diameter and length of the CO_2 sorbent bed are 8" and 12" respectively.

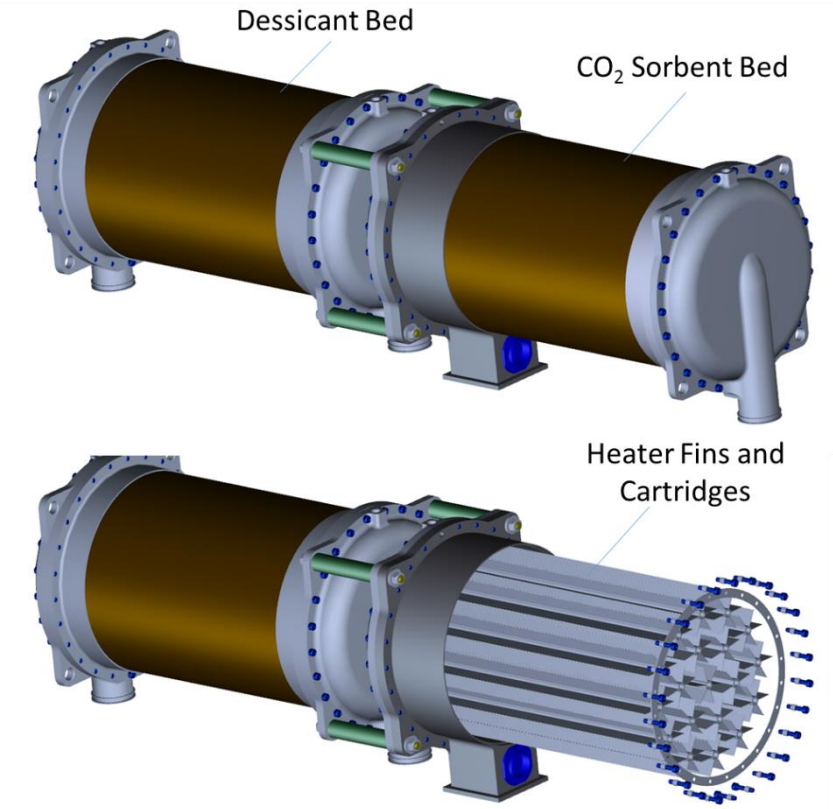

Figure 2. 4BMS-X

An individual heater core is shown in Figure 3. The core is comprised of a heater cartridge mounted into a six point fin assembly. Each fin assembly is constructed from Aluminum 6061-T6 with dimensions as shown in the figure. The individual fins are tapered with a greater thickness at the base. The assembly has a 0.25" penetration in the base to accommodate a cartridge heater. The fins are placed as shown within the sorbent bed. The heater core assemblies are 12" in length. There is some additional sorbent at the end of the sorbent bed opposite the desiccant bed coupling to completely cover the heater cores.

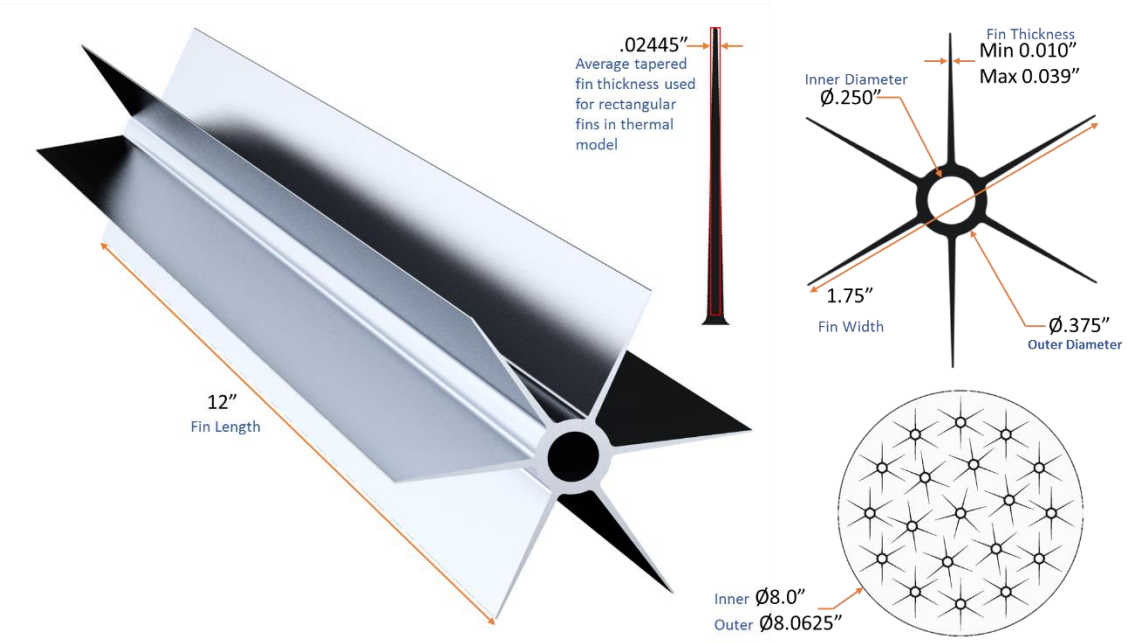

Figure 3. 4BMS-X Heater Fin Placement and Sizing

The heater cores are mounted into an Inconel end plate. The end plate is produced through an additive manufacturing process with a lattice filled spacing between cartridge heater mounting holes as shown in Figure 4. The lattice provides structural strength while minimizing thermal conductivity (due to the void space inside the lattice). The end plate mounts on a flange inside one of the 4BMS-X sorbent bed end caps as shown in the figure.

Figure 4. 4BMS-X Heater Mounting Plate and Sorbent End Cap

III. Trade Space

Two additional heater core arrangements were considered for the trade study. A cross section of the cylindrical 4BMS-X CO2 sorbent bed with each arrangement is provided in Figure 5. The spiral configuration is composed of a Kapton heater sandwiched between two aluminum face sheets formed in the shape of an Archimedes spiral. Four spirals are arranged to provide an approximate spacing throughout the bed such that the sorbent is a prescribed distance

away from any heated surface. The spirals are truncated short of the external container to minimize heat leak so the spacing is not preserved at the boundaries. The second heater core arrangement (baseline) is composed of cartridge heaters embedded inside of tapered aluminum star shaped fins spaced 60° apart (see Figure 5). The heaters and fin assemblies are spaced evenly inside of the sorbent bed with twelve heaters around the periphery and seven in the center (for a total of 19 heaters). The sorbent material fills the void spaces created by the fins and outer container. The heaters are attached to a mounting plate at one end of the sorbent bed. Initially constructed from Aluminum 6061, the heater mounting plates will be fabricated from titanium or Inconel with a specially machined or additive manufactured interface flange designed to minimize heat leak through the end cap. The final option utilizes similar heater cores and fins but arranged in the organized pattern shown in the figure. The fin assemblies don't actually touch and are arranged to created small triangular voids filled with sorbent inside of a large hexagonal pattern. All points within the bounding hexagon are within 0.5" of a heater surface. In order to produce the structured arrangement three different parts are utilized with 3, 4 or 6 fins (blue, red and orange respectively) attached to a cartridge assembly. The three heater core arrangements are considered for down select to a single option for more detailed modeling and test evaluation.

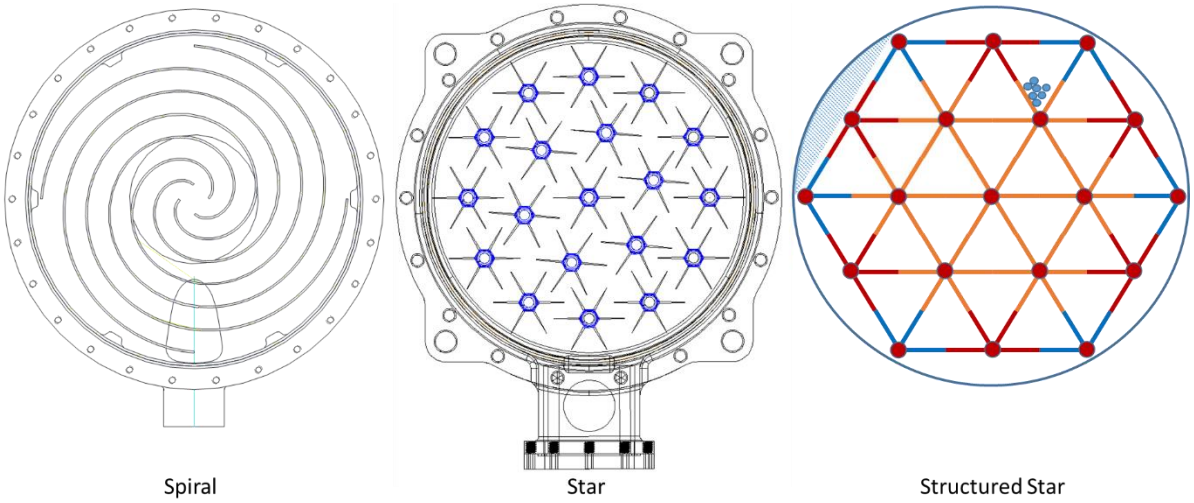

Figure 5. 4BMS-X Heater Configuration Option

Bed characteristics, based on geometry and scaled for a full size bed, are provided in Table 1. Owing to thin sheets and Kapton heaters, the spiral sheet option presents the minimum volume and maximum surface area for any of the options considered. Because of the small volume, the spiral sheet option also minimizes heater assembly mass and thermal mass. Thermal mass is based on the product of specific heat and mass of the heater materials which prescribes the amount of energy required to raise the heater one degree in temperature. The specific heats are averaged over the expected operating interval (20°C to 200°C) during the initial half cycle ramp. As shown in the table, the sorbent mass fraction describes the ratio of sorbent to total mass (not including the container). But the heater and container represent a significant thermal mass as the ratio of sorbent thermal mass to total mass is generally below 70% for the star shaped fin options. Accounting for the container thermal mass, the sorbent thermal mass fraction is 78% for the spiral fin option.

Table 1. 4BMS-X Bed Characteristics

	Spiral	Star	Structured Star
Sorbent Volume Fraction	97.3%	92.6%	93.6%
Sorbent Mass Fraction	93.8%	70.9%	72.8%
Sorbent Thermal Mass Fraction (no Container)	89.2%	69.8%	72.4%
Sorbent Thermal Mass Fraction (with Container)	78.0%	62.7%	64.9%
Heater Core Mass (kg)	0.70	3.26	2.97
Heater/Fin Surface Area (m^2)	1.31	0.82	0.65

IV. Model Approach and Development

2D and 3D thermal models of the 4BMS-X CO_2 sorbent bed are developed within the Cullimore and Ring Technologies Thermal Desktop® [4] application. The 2D model is based on a representative cross sectional slice through the sorbent bed and is utilized to optimize heater sizing and fin thickness. The sorbent material is modeled as a homogeneous mixture of solid sorbent pellets and CO_2 gas nominally at 1 psia pressure. The actual pressure is only important in that continuum assumptions may be applied for the small voids created by pellet to pellet or pellet to wall contact within the sorbent volume. Temperature varying thermo-physical properties (k, c_p) as well as density are obtained by direct measurement under nitrogen for the zeolite 13X sorbent[5] (from industry data) and converted to CO_2 via the Krupiczka[6] relation. Boolean operations on CAD geometry of the cylindrical sorbent bed are used to create a model of the sorbent volume for meshing. After subtracting the heater cartridge and fin assembly volumes from inside the bed volume defined by the outer container, the sorbent space is discretized into triangles for the 2D model (see Figure 6). The triangles are subsequently extruded along the long axis of the sorbent bed to form finite element wedges for the 3D model. The star shaped heater fin assemblies are modeled using Thermal Desktop cylinder and rectangle primitives and inserted into the appropriate voids within the 2D or 3D sorbent mesh. The primitives allow for easy parameterization of several geometric properties including fin thickness and heater power. An average thickness is assumed for tapered fins. The fins and heaters are ideally coupled via corresponding nodes in Thermal Desktop. A contact conductance is applied between the star shaped fins and the sorbent as detailed in a subsequent section.

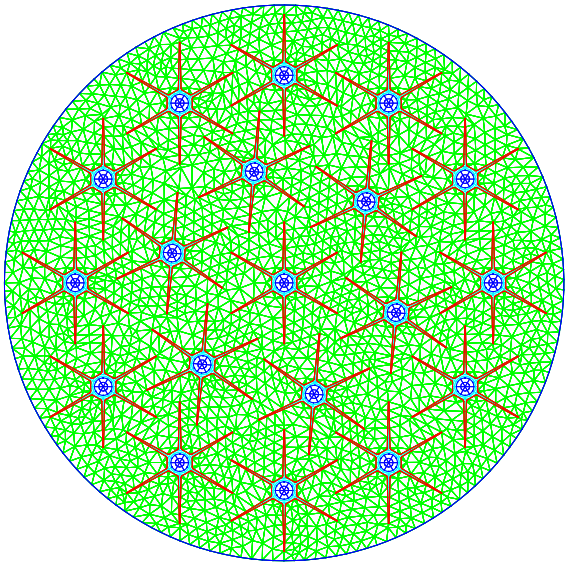

Figure 6. 2D 4BMS-X Sorbent Model. *The green triangles represent the sorbent mesh. Heater cartridges are the blue cylinders with fins in red/cyan.*

For the 3D model, the barrel section is also modeled using a Thermal Desktop cylinder primitive while the end caps and flanges are created as surfaces of revolution based on the original CAD geometry (see Figure 7). An ideal contact conductance (i.e. correspondence) is assumed for the bolted flange to end-cap interface and the sorbent bed is coated with a thermal resistance representing ¾" of Pyropel LD-6 insulation followed by a free convection coefficient to the surrounding environment at standard atmospheric conditions. The end-caps are simplified with no connection to adjoining hardware. The adiabatic end conditions may be changed in a future revision of the model if heat leak to external hardware is found to be significant through correlation to test data.

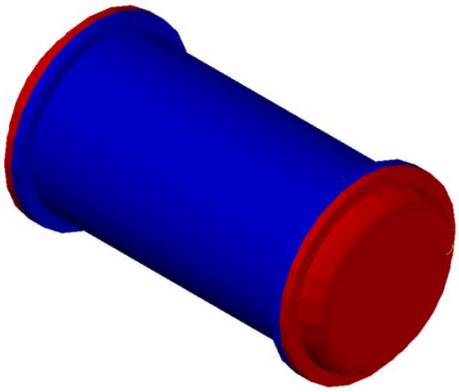

Figure 7. 3D 4BMS-X External Model. *The barrel section and flanges are in blue while the end-caps are red.*

The internal 4BMS-X Thermal Desktop 3D model is shown in Figure 8. The sorbent volume (yellow) is discretized into finite element wedges derived from the mesh generated for the 2D model. The voids for the heater cartridges and star shaped fins are evident in the graphic. The sorbent volume fits inside the external container model with a thermal contact coupling between the sorbent and container. Likewise, the heater assembly fits within the sorbent model with a contact coupling between the fins and the sorbent. The model contains over 50,000 nodes with execution times on the order of 5 minutes for a transient 60 minute simulation.

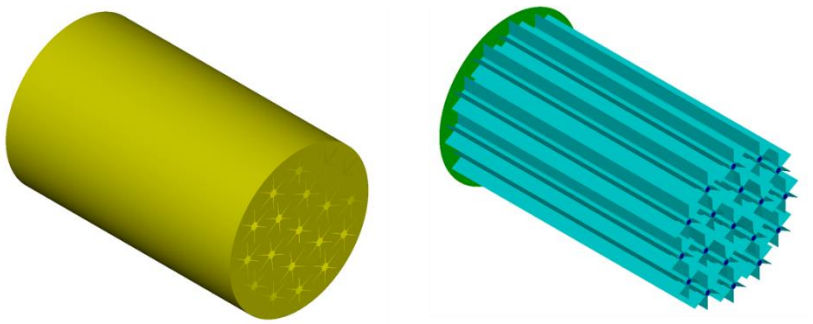

Figure 8. 3D 4BMS-X Internal Model. *The core sorbent elements are in yellow while the heater fins are cyan. The heater mounting plate is green.*

Perhaps the most important facet of each model is the determination of the contact conductance between the fin/container walls and the sorbent/gas mixture. A representation of the interface between a fin (wall) and sorbent is shown in Figure 9. At the fin surface, the void fraction of the sorbent bed is 100% as any spherical pellets contacting the wall do so only at a tangent point. Moving perpendicularly away from the wall, the average void fraction will decrease and spatially average thermal properties will increase to the bulk values in the bed after some interface distance. Exactly at the wall, the thermal conductivity, density and specific heat of the sorbent/gas mixture will be defined only by the gas and then by the relative contributions of each phase thereafter. The governing equation for time dependent conduction heat transfer in the bed volume up to the wall interface boundary is based on the thermal diffusivity of the gas/solid mixture.

A modeling approach is implemented for heater/sorbent coupling where a thin interface region (of high diffusivity) near the wall is simply modeled as a thermal resistance with bulk properties used deeper in the bed. The thin interface region doesn't participate in energy storage (since the thermal diffusivity, α, of the gas is much greater than the solid) but the thermal coupling is modeled via boundary condition or thermal contact.

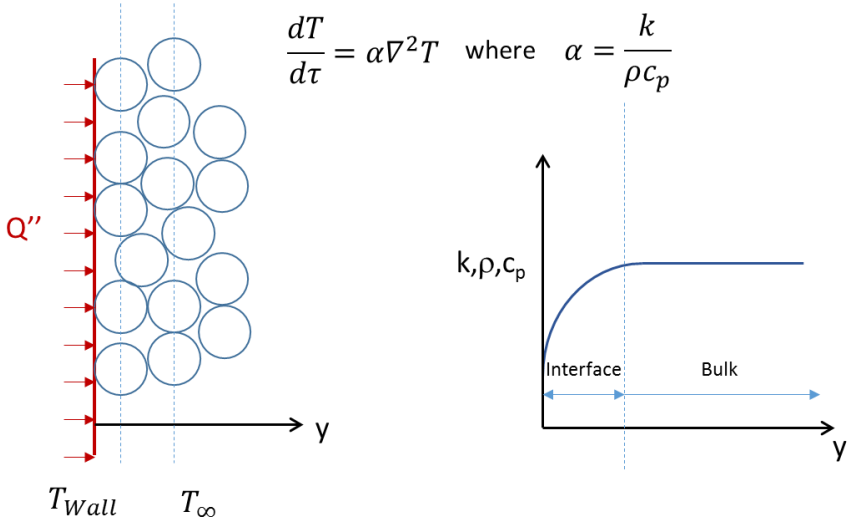

Figure 9. Thermal Diffusivity versus Relative Distance from Wall.

A relationship defining the void fraction as a function of relative distance (normalized by the pellet diameter) from the wall is provided in Equation 1.[7]

$$\varepsilon = \varepsilon_\infty \left[1 + C exp\left(-N\frac{y}{d_p}\right)\right] \quad (1)$$

The constant C is adjusted to provide the proper void fraction at the wall given the desired bulk void fraction while N is based on empirical observation (N=2…8).[8] For this application the lowest value of N is chosen for conservatism (i.e. highest void fraction=lowest contact conductance). The bulk void fraction of the sorbent is 0.41 (based on measurement) so C is derived to be 1.439 (i.e. [1- ε_∞]/ ε_∞). The variation of the void fraction versus relative distance from the wall is provided in Figure 10.

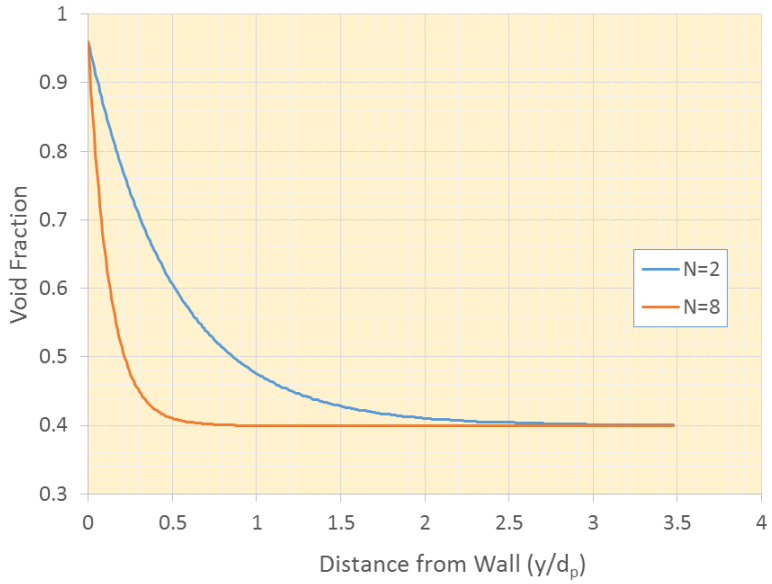

Figure 10. Void Fraction versus Relative Distance from Wall.

Assuming that the variation of thermal conductivity in the interface region is proportional to the void fraction, then thermal diffusivity as a function of distance from the wall can be derived as shown in Figure 11. The thermal diffusivity is expressed as a relative ratio to the solid sorbent and approaches bulk values within a half of a pellet diameter from the wall over the range of permissible multiplication factors.

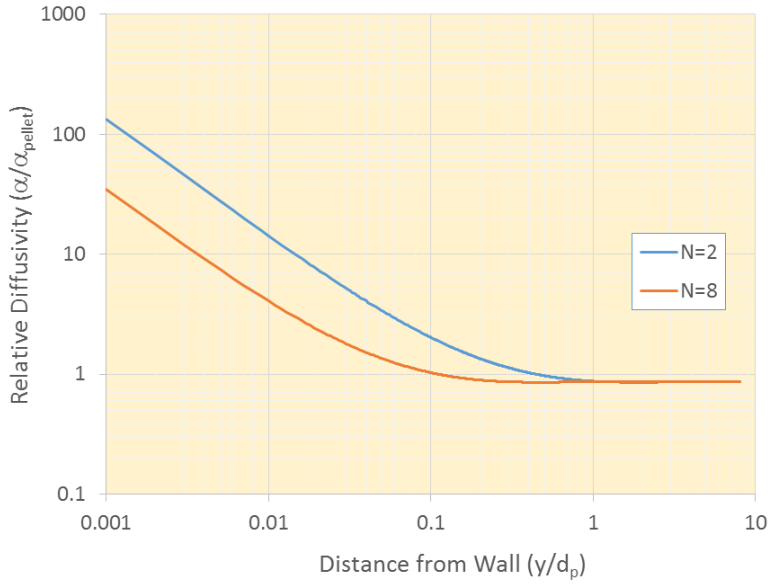

Figure 11. Thermal Diffusivity versus Relative Distance from Wall.

An overall heat transfer coefficient at the wall (fin surface) is derived from the Fourier 1D heat conduction[9] equation (2) which is integrated to determine an equivalent heat conduction coefficient (or effective thermal

conductivity) over the depth of the interface layer denoted as L (see equations 3 through 6). The temperature of the wall is denoted as T_{wall} and the temperature of the sorbent a distance L away from the wall is denoted T_{∞}. The thermal conductivity, k, is scaled over the depth of the interface layer as a volume average of the sorbent thermal conductivity and the gas conductivity. The final result is shown in equation 6 with the thermal coupling expressed as a convective heat transfer coefficient, h, or an effective thermal conduction k_{eff} (which includes both solid and gas).

$$Q'' = -k\frac{dT}{dx} \tag{2}$$

$$Q''\int_0^L \frac{dx}{k} = -\int_{T_{Wall}}^{T_\infty} dT \tag{3}$$

$$Q'' = \left(\int_0^L \frac{dx}{k}\right)^{-1}(T_{Wall} - T_\infty) \tag{4}$$

$$Q'' = h(T_{Wall} - T_\infty) \tag{5}$$

$$h = \left(\int_0^L \frac{dx}{k}\right)^{-1} \text{ or } \quad k_{eff} = L\left(\int_0^L \frac{dx}{k}\right)^{-1} \tag{6}$$

The computed result for the fin to sorbent contact coefficient versus temperature is shown in Figure 12 for zeolite 13X under CO_2.

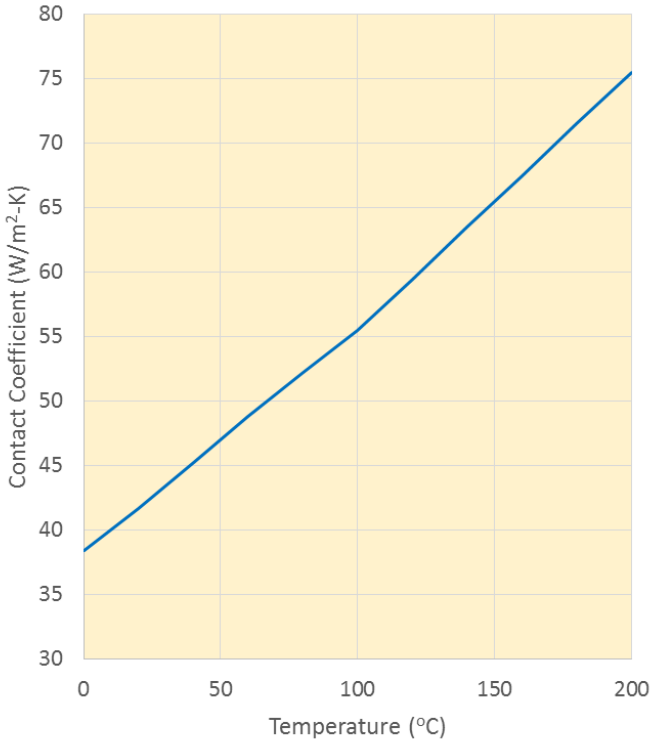

Figure 12. 13X Effective Wall Contact Conductance (CO_2).

V. Model Results

Cross sectional bed temperature profiles for each of the three options considered in the previous trade are provided in Figure 13. A dual heater zone control option is largely responsible for the improved isothermal temperature distribution of the star shaped fin arrangement. The spiral and structured star options have difficulty maintaining temperatures near the boundary. Lengthening the spirals or expanding the hexagonal fin boundary may result in improved performance for those options.

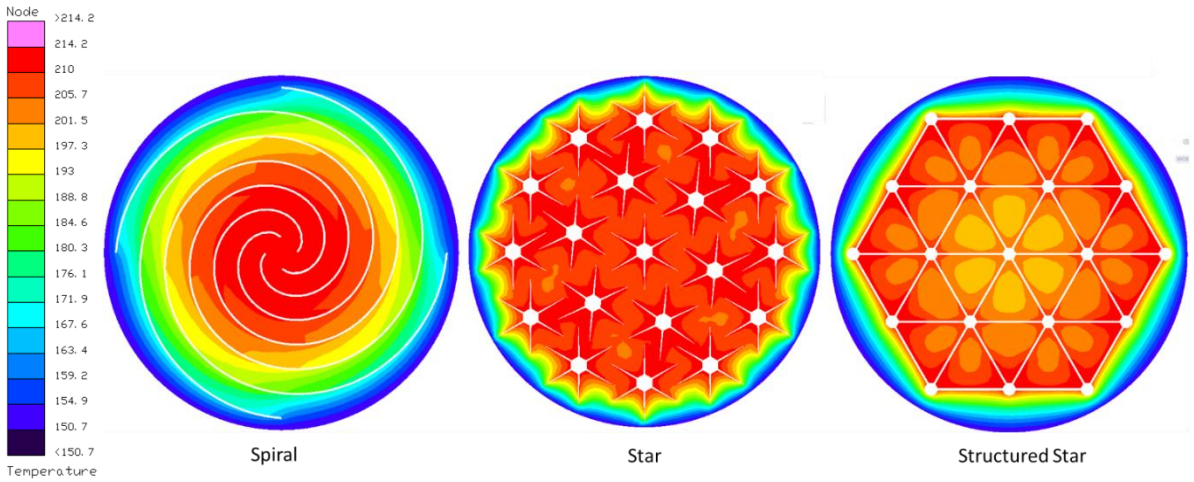

Figure 13. 4BMS-X Heater Configuration Options

A summary of bed gradient and heater power for the three options is presented in Table 2. For maintaining an isothermal bed, the well distributed star fin assembly outperforms the other two options (as evidenced by the T_{max}-T_{min} metric). The spiral heater sheet option only utilized a single heater zone and it is expected that a multi-zone approach could improve the spiral heater bed gradient and potentially make this option a more competitive approach; but ultimately the spiral configuration was eliminated due to the lack of a suitable high temperature adhesive to bond the face sheets to the Kapton heater core. Some heater anomalies in the ISS CDRA were attributed to poor contact between the heaters and spreader plates which resulted in hot spots. For the structured star, there is concern about the fin tips between neighboring stars not joining exactly and creating small gaps that would increase channeling. Although both options were eliminated for non-thermal reasons, the analysis provided useful performance insight and a possible path to future upgrades. The well distributed star fin assembly is chosen for the baseline configuration.

Table 2. 4BMS-X Heater Options

	Spiral	Star	Structured Star
T_{max}-T_{min} (°C)	64	47	67
Heater Power (watts)	240	414	413

2D 4BMS-X model parametric results for average sorbent bed temperature versus fin thickness (relative to cartridge heater power) are shown in Figure 14. The average sorbent bed temperature is determined for a 60 minute heating interval. The average sorbent bed temperature decreases with increasing fin thickness due to added thermal mass resulting from a larger fin. Three power levels are shown with the current baseline fin thickness (0.62 mm). Points A, B and C represent the design condition to meet the desired average sorbent bed temperature of 200°C for each of the power levels. The figure shows how important it is to match the fin thickness to the power level for a desired target temperature. Larger fins aren't necessarily beneficial since, with both a target temperature and time requirement, a larger fin will require longer to heat up.

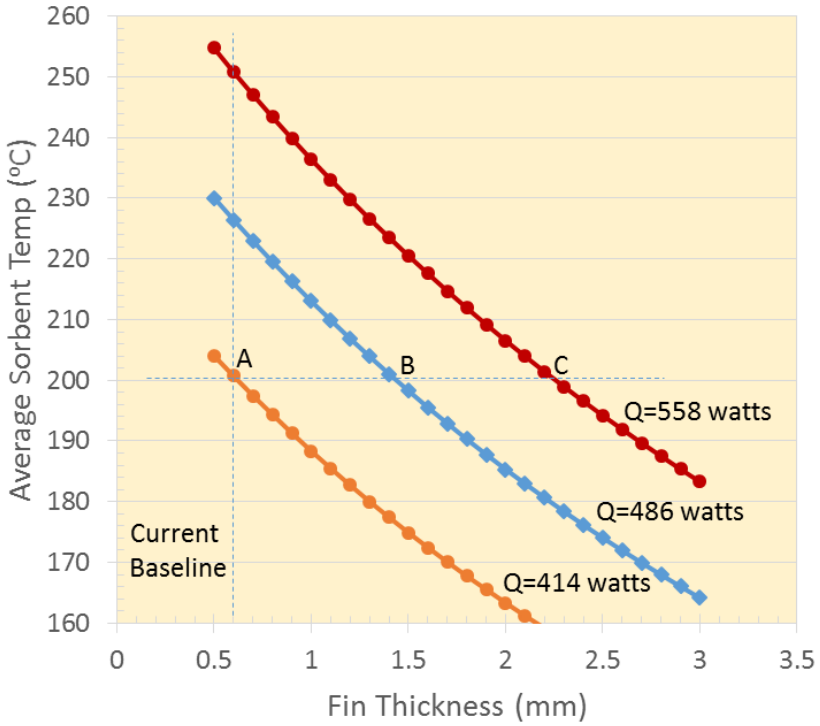

Figure 14. 4BMS-X Fin Thickness Parametric

Is there an optimum fin thickness to meet both the time and target temperature requirement? For an isothermal bed there does appear to be an optimum fin thickness as shown in Figure 15. Using the power required to produce an average sorbent bed temperature of 200°C in 60 minutes the curve below is produced containing an inflection point. Operating points A, B and C are noted in the plot. The inflection point represents the minimum bed gradient and illustrates the competition between fin thickness, fin thermal mass and the contact coupling from the fin to the bed. Below the inflection point (thin fin) the fin conductance is the limiting factor and increasing the fin thickness is beneficial (to a point). Above the inflection point (thick fin) the thermal mass of the fin becomes significant as the large amount of energy required to raise the fin temperature cannot effectively be transmitted to the bed due to the limited contact conductance to the sorbent. The limited heat transfer to the sorbent is shown in Figure 16 as the heater core temperature rises despite the increased thermal mass of the fin. It appears that the optimum thickness for the star shaped fins is about 1 mm.

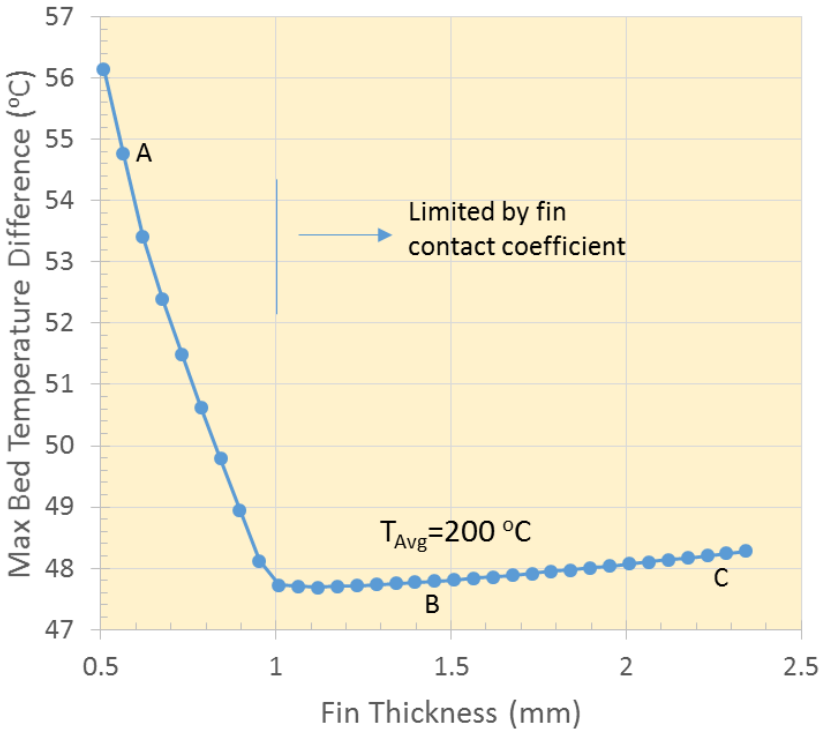

Figure 15. 4BMS-X Isothermal Bed Parametric

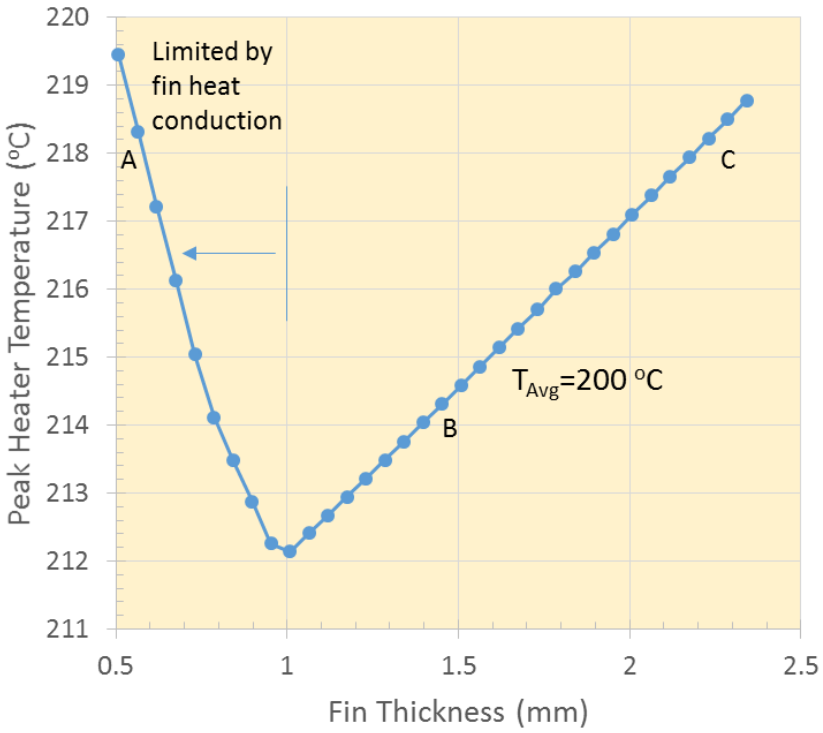

Figure 16. 4BMS-X Peak Heater Core Temperature

The temperature profile through a 2D slice of the sorbent bed at the optimized fin thickness and cartridge power is shown in Figure 17. The peak temperature of the sorbent is 208 ºC with a gradient to the external wall at 160 ºC. Aside from the gradient at the boundary, the bed is largely uniform in temperature. Further optimizations involving insulation thickness and fin placement may enhance the result.

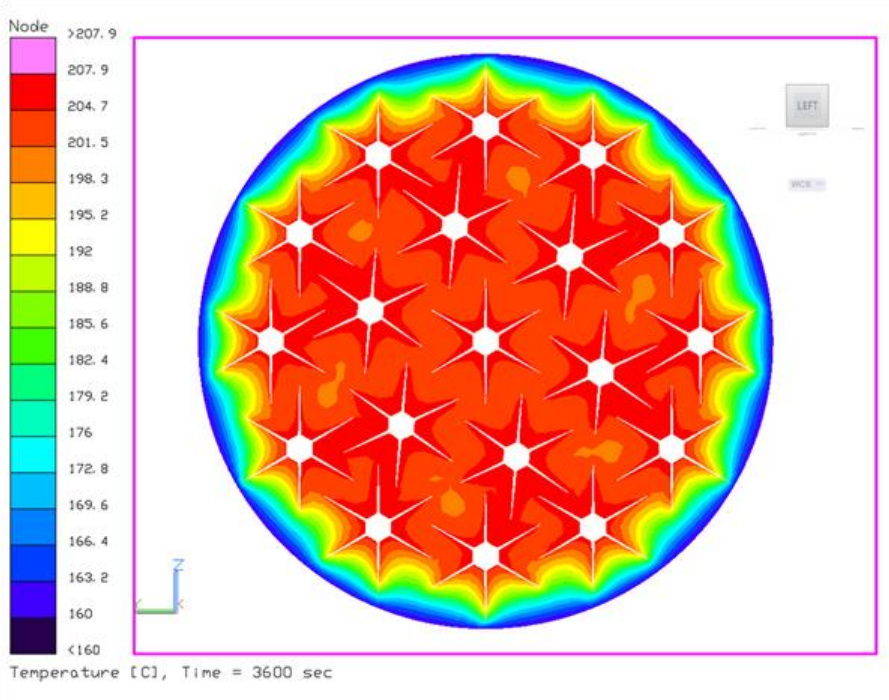

Figure 17. 2D Sorbent Bed Temperature Profile (1mm Heater Fins).

3D 4BMS-X analysis predictions for the heater core are shown in Figure 18. A small axial gradient due to heat leak through the heater/fin attachment to the mounting plate is evident in the profile. Lattice sections of the Inconel mounting plate are removed from the plot for clarity. The mounting plate is coupled to the aft flange of the external container end cap. In addition to the lower effective thermal conductance achieved through additive manufacturing processes and the usage of favorable materials like Inconel, mitigation strategies to reduce the gradient also include thermal isolation between the fin/cartridge assemblies and the mounting plate and from the mounting plate to the external flange.

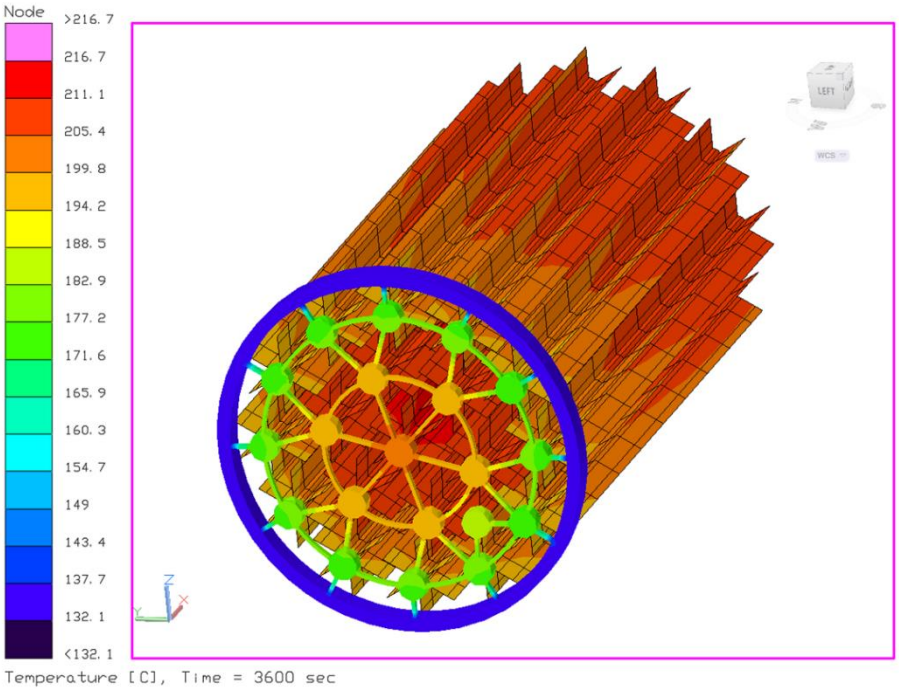

Figure 18. 3D Sorbent Bed Heater Core Temperature Profile.

Thermal gradients in the external canister are evident in Figure 19 due to the internal attachment of the heater core to the external flange. The attachment (aft) end is warmer than the opposite end but a peak in the barrel temperature also indicates heat conduction directly from the sorbent bed into the container wall. Reduction of the heat leak will result in improved efficiency.

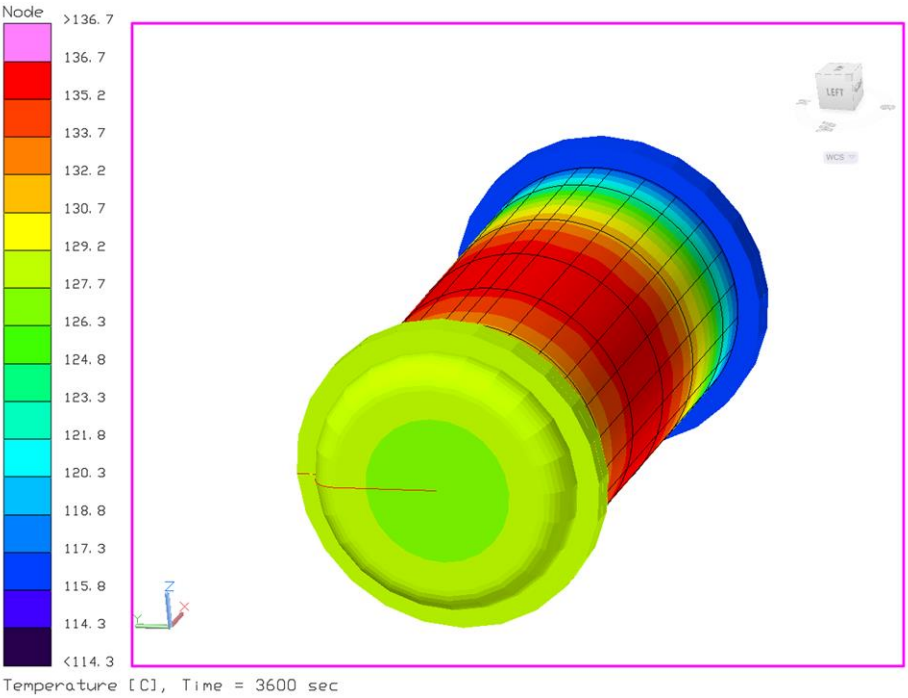

Figure 19. 3D Sorbent Bed External Canister Temperature Profile.

VI. Discussion

A design and heater optimization study for 4BMS-X CO_2 sorbent beds in a proposed exploration system architecture has been completed. Three heater concepts were considered in the initial study via two dimensional models to assess thermal gradient and heater performance within a cross-section of the bed. A baseline concept, composed of cartridge heaters embedded inside of tapered aluminum star shaped fins, was established for continued development. Although the modeling effort yielded valuable insight on the thermal performance of all of the concepts, two of the options were eliminated due to concerns about channeling and the availability of a high temperature adhesive.

An analytical approach to predict the contact conductance between sorbent materials and solid surfaces based on empirical void fractions was developed and employed in both the 2D and 3D models used in this study. Given the heater fluxes necessary to achieve desired ramp rates, the predicted contact conductance appears sufficient to prevent large gradients between heater fin and sorbent.

Two dimensional models of the baseline concept with roughly equidistant cartridge heaters/fins show thermal gradients confined mostly to the edges of the circular container with a roughly isothermal center section. Parametric studies with the two dimensional models show an optimum fin thickness with respect to gradient and heater power. Future designs may benefit from this optimization.

Three dimensional thermal models of the baseline concept identified axial thermal gradients caused by heat loss through a conductive heater mounting plate. Additive manufacturing of the end plate to produce custom geometries may be used to further reduce the thermal gradient. Because of the desired ramp rate for desorption, the impact of the relative thermal masses of the sorbent, container and heater core on performance is evident in the results.

VII. Future Plans

Thermal model correlation to test data will be the highest priority for future work. Thermal tests of a developmental 4BMS-X CO2 sorbent bed will be invaluable for substantiating model predictions regarding axial and radial sorbent bed thermal gradients, heater power and transient thermal performance. Various assumptions about contact conductance's and effective sorbent thermal conductance developed for the thermal model will be validated to the extent possible through test.

Further refinement of 4BMS-X thermal models are anticipated to support future design activities. The modeling will support design enhancements to reduce both radial and axial thermal gradients and minimize heater power.

Acknowledgments

The authors wish to acknowledge to contributions of the ISS Program and AES LSS Project in sponsoring this work and for the many useful suggestions and discussions provided by the CO_2 Removal Simulation and CO_2 Removal Roadmap and Sorption teams.

References

[1] Knox, J. C.; Watson, D. W.; Giesy, T. J.; Cmarik, G. E.; Miller, L. A. Investigation of Desiccants and CO2 Sorbents for Exploration Systems 2016-2017, In 47th International Conference on Environmental Systems, Charleston, 2017.

[2] Brown, Arthur, "Particle Size Analysis: Grade 544, ASRT 2005", NASA/MSFC, 2017.

[3] "Pyropel Physical Properties - Metric", Grace Materials Technologies, Albany International, Rochester, NH, URL: http://www.albint.com/business/pyropel/Data%20Sheet/Physical%20Properties%20Metric.pdf.

[4] Thermal Desktop, PC/CAD-based thermal model builder, Software Package Ver. 5.8, Cullimore and Ring Technologies, Littleton, CO, 2016.

[5] Kay, Robert and Pancho, Donna, "Evaluation of Alternative Desiccants and Adsorbents for the Desiccant/Adsorbent Bed, PN 2352540-1-4 International Space Station Purchase Contract Number: 458314", 12-77742, January 25, 2013.

[6] R. Krupiczka, Analysis of thermal conductivity in granular materials, Int. Chem. Eng. 7, 122-144 (1967).

[7] Cheng, P.; Chowdhury, A.; Hsu, C. T. Forced Convection in Packed Tubes and Channels with Variable Porosity and Thermal Dispersion Effects. In Convective Heat and Mass Transfer in Porous Media, Kakaç, S.; Kilkiş, B.; Kulacki, F. A.; Arinç, F., Eds. Springer Netherlands: Dordrecht, 1991; pp 625-653.

[8] Nield, D. A.; Bejan A.; Convection in Porous Media, Third Edition, Springer Science and Business Media, 2006, pp 22.

[9] Welty, J.; Wicks, C. E.; Wilson R.E.; Fundamentals of Momentum, Heat and Mass Transfer, 2nd Edition, Wiley, 1976.